Check for updates

Reduction of silver nanoparticle toxicity affecting ammonia oxidation using cell entrapment technique

Nguyen Thanh Giao, Tawan Limpiyakorn, Pumis Thuptimdang, Thunyalux Ratpukdi and Sumana Siripattanakul-Ratpukdi

ABSTRACT

Occurrence of silver nanoparticles (AgNPs) in wastewater treatment systems could impact the ammonia oxidation (AO). This study investigated the reduction of AgNPs and dissociated silver ion (Ag^+) toxicity on nitrifying sludge using cell entrapment technique. Three entrapment materials, including barium alginate (BA), polyvinyl alcohol (PVA), and a mixture of polyvinyl alcohol and barium alginate (PVA-BA), were applied. The BA beads provided the highest reduction of silver toxicity (up to 90%) and durability. Live/dead assays showed fatality of entrapped cells after exposure to AgNPs and Ag^+. The maximum AO rate of the BA-entrapped cells was 5.6 mg-N/g-MLSS/h. The AO kinetics under the presence of silver followed an uncompetitive inhibition kinetic model. The experiments with AgNPs and Ag^+ gave the apparent maximum AO rates of 4.2 and 4.8 mg-N/g-MLSS/h, respectively. The apparent half-saturation constants of the BA-entrapped cells under the presence of silver were 10.5 to 13.4 mg/L. Scanning electron microscopic observation coupled with energy-dispersive X-ray spectroscopy indicated no silver inside the beads. This elucidates that the silver toxicity can be reduced by preventing silver penetration through the porous material, leading to less microbial cell damage. This study revealed the potential of the entrapment technology for mitigating the effect of silver species on nitrification.

Key words | entrapped cells, nitrifying activated sludge, silver nanoparticles

Nguyen Thanh Giao
International Program in Hazardous Substance and Environmental Management, Graduate School,
Chulalongkorn University,
Bangkok 10330,
Thailand
and
Department of Environmental Management,
College of Environment and Natural Resources,
Can Tho University,
Can Tho 90000, Viet Nam

Nguyen Thanh Giao
Tawan Limpiyakorn
Thunyalux Ratpukdi
Sumana Siripattanakul-Ratpukdi (corresponding author)
Center of Excellence on Hazardous Substance Management,
Bangkok 10330, Thailand
E-mail: *sumana.r@kku.ac.th*; *jeans_sumana@yahoo.com*

Tawan Limpiyakorn
Department of Environmental Engineering, Faculty of Engineering and Research Unit Control of Emerging Micropollutants in Environment,
Chulalongkorn University,
Bangkok 10330, Thailand
and
Research Network of Chulalongkorn University and National Nanotechnology Center (RNN),
Bangkok, Thailand

Pumis Thuptimdang
Department of Chemistry, Faculty of Science and Environmental Science Research Center (ESRC),
University of Chiang Mai,
Chiang Mai 56000, Thailand

Thunyalux Ratpukdi
Sumana Siripattanakul-Ratpukdi
Department of Environmental Engineering, Faculty of Engineering and Research Center for Environmental and Hazardous Substance Management,
Khon Kaen University,
Khon Kaen 40002, Thailand

INTRODUCTION

Silver nanoparticles (AgNPs) have been used in many applications, such as textile, medical, and plastic products (Pantic 2014). The large amount of AgNPs used resulted in residue being deposited in wastewater treatment plants (WWTPs) (Mitrano *et al.* 2011; Hoque *et al.* 2012; Li *et al.* 2013). With the superior antimicrobial ability of the particles, microorganisms in WWTPs, including nitrifying microorganisms, might be inhibited (Chopra 2007). Previous works reported

doi: 10.2166/wst.2019.075

Downloaded from http://iwaponline.com/wst/article-pdf/79/5/1007/618293/wst079051007.pdf
by guest

that ammonia oxidation (AO) activity of nitrifying sludge could be seriously inhibited by silver species, including AgNPs and liberated Ag^+ (Choi *et al.* 2008; Jeong *et al.* 2012; Giao *et al.* 2017). The silver species that partially inhibited the AO process followed uncompetitive inhibition-like kinetics with the AgNPs and liberated Ag^+ inhibitory constants of 73.5 and 0.29 mg/L, respectively (Giao *et al.* 2017).

The potential of the cell entrapment technique to alleviate the negative impact of toxic substances on microbial activity has been studied. Cell entrapment materials reduce cell exposure to toxic chemicals leading to lower microbial inhibition (Saez *et al.* 2012; Siripattanakul-Ratpukdi 2012; Siripattanakul-Ratpukdi *et al.* 2014; Lucchesi *et al.* 2015). Prior studies have also indicated that the entrapment materials assist living microorganisms to resist adverse environmental conditions (e.g. pH and temperature changes) and to retain higher cell numbers in the system without reducing the microbial activity (Siripattanakul & Khan 2010; Hu & Yang 2015). Siripattanakul-Ratpukdi *et al.* (2014) found much lower inhibition of nitrification in the entrapped cell system influenced by AgNPs. The previous work preliminarily proved the feasibility of the entrapped cell application. However, the treatment performance and the durability of entrapped cells depended on the entrapment materials (Paul & Vignais 1980; Liu *et al.* 2012). For example, changing salt solutions (from calcium chloride to barium chloride) during the preparation of gel beads could significantly improve the physical and chemical properties. This, in turn, could lead to higher yield and activity of the entrapped cells (Paul & Vignais 1980). The addition of sodium alginate to polyvinyl alcohol (PVA) could also enhance the stability of the produced beads (Liu *et al.* 2012).

This study investigated the reduction of AgNP toxicity affecting AO using cell entrapment techniques. The screening of the entrapment materials (barium alginate (BA), polyvinyl alcohol (PVA), and mixture of polyvinyl alcohol and barium alginate (PVA-BA)) was based on nitrification performance and bead durability. The influence of silver species (AgNPs and Ag^+) on the inhibition of AO was evaluated. The AO kinetics of selected entrapped cells were also investigated. Microbial cell viability and morphology were observed by confocal laser scanning microscopy (CLSM) and scanning electron microscopy coupled with an energy dispersive X–ray (SEM-EDX). This primarily elucidated the mechanism of silver toxicity reduction. The results of this study could be used as fundamental information for AgNP contaminated wastewater treatment in the future.

MATERIALS AND METHODS

AgNPs and Ag^+

Silver nanoparticles (5,000 mg/L) were obtained from PrimeNANO technology (Prime Nanotechnology Co. Ltd, Chulalongkorn University, Thailand). Transmission electron microscopy showed spherical AgNP sizes in the range of 2–12 nm (Giao *et al.* 2017). AgNP suspensions prepared in inorganic synthetic wastewater (SWW) peaked at a wavelength of 400 nm, which indicated that AgNPs were well dispersed in the experimental condition. Additionally, the residue of Ag^+ from AgNPs of 10 mg/L was found to be less than the method detection limit (3 μg/L). Silver nitrate ($AgNO_3$, Merck, Darmstadt, Germany) was used as a source of Ag^+.

Nitrifying sludge acclimation

The seed sludge was taken from a continuous-flow enriching nitrifier reactor. The continuous reactor had been operating for more than five years with equal hydraulic (HRT) and solid (SRT) retention times of four days. During nitrifying sludge acclimation, SWW was comprised of 1.9821 g/L $(NH_4)_2SO_4$, 0.2 g/L NaCl, 0.2 g/L K_2HPO_4, 0.4 g/L $MgCl_2.6H_2O$, 0.1 g/L $CaCl_2.2H_2O$, 0.5 g/L KCl, and 1.0 g/L $NaHCO_3$ with an addition of 1 mL of inorganic salt solution. The inorganic salt solution contained 40 g/L $MgSO_4.7H_2O$, 40 g/L $CaCl_2.2H_2O$, 200 g/L KH_2PO_4, 1 g/L $FeSO_4.7H_2O$, 0.1 g/L Na_2MoO_4, 0.2 g/L $MnCl_2.4H_2O$, 0.02 g/L $CuSO_4.5H_2O$, 0.1 g/L $ZnSO_4.7H_2O$, and 0.002 g/L $CoCl_2.6H_2O$. The NH_4^+-N concentration of 429 ± 62 mg-N/L was maintained. For the silver exposure experiment, wastewater was comprised of 1.9821 g/L $(NH_4)_2SO_4$, 1 g/L $NaHCO_3$, 0.1 g/L K_2HPO_4, 0.025 g/L $MgSO_4$, and 0.025 g/L NaCl with AgNPs and Ag^+ at 10 mg/L and 0.1 mg/L, respectively.

Entrapped cell preparation

The enriched nitrifying sludge was harvested and centrifuged at 5,000 rpm for 20 min and the clear supernatant was removed. The concentrated cells were re-suspended, well-mixed, and centrifuged in SWW as a washing process five times. The washed cells were used for preparing the entrapped cells. The washed cells were added to the entrapment matrices to reach a final cell concentration in the matrix of 2,000 mg-MLSS/L.

Downloaded from http://iwaponline.com/wst/article-pdf/79/5/1007/618293/wst079051007.pdf
by guest

Preparation of the BA and PVA-entrapped cells followed previous works (Siripattanakul-Ratpukdi & Tongkliang 2012; Siripattanakul-Ratpukdi *et al.* 2014). To prepare BA-entrapped cells, 2% (w/v) alginic acid sodium salt and 5% (w/v) barium chloride were used. The alginic acid sodium salt solution and the nitrifying sludge were homogeneously mixed and then dropped into the barium chloride solution using a peristaltic pump at 20 rpm. The gel beads were hardened in the barium chloride solution for 1 h. BA gel beads with diameters of 3–6 mm were formed.

For the PVA-entrapped cells, 10% (w/v) polyvinyl alcohol (PVA, 99%, fully hydrolyzed) was applied. The mixture of the PVA solution and the nitrifying sludge was dropped into a saturated boric acid solution for 30 min before it was transferred to a 1 M sodium phosphate buffer for 2 h to harden the produced gel beads. PVA gel beads of 3–6 mm diameters were formed. The other entrapment material applied in this study was a PVA-BA matrix. The combination of PVA and alginate was developed and successfully applied for entrapping phenol-degrading bacteria (Wu & Wisecarver 1992). The PVA-BA-entrapped cells were prepared by using 10% (w/v) polyvinyl and 1% (w/v) alginic acid sodium salt. The combined gel solution was mixed with the sludge. The preparation protocol for PVA-BA-entrapped cells followed that of the PVA gel, as described above.

Experimental setup and procedure

AO batch experiments were performed. A glass reactor with 100 mL working volume was applied. The reactor was operated under room temperature and 2 mg/L dissolved oxygen (DO). The study was divided into two parts: (1) inhibited AO by entrapped cells and (2) kinetics of AO by selected entrapped cells. The first part emphasized on selection of appropriate entrapment material (among BA, PVA, and PVA-BA) for the situation. The selection was based on AO percentage, bacterial viability, and material durability. For the second part, AO kinetics by selected entrapped cells was performed. This part focused on AO modeling based on Monod equation. Also, bacterial cell and bead morphology after the experiment was investigated using SEM-EDX. Figure 1 is summarized overall experiments.

Inhibited AO by entrapped cells

AO experiments on free cells, entrapped cells, and only materials were performed under the absence and presence of silver species. NH_4^+-N, Ag^+, and AgNP concentrations of 70, 0.1, and 10 mg/L, respectively, were applied. The

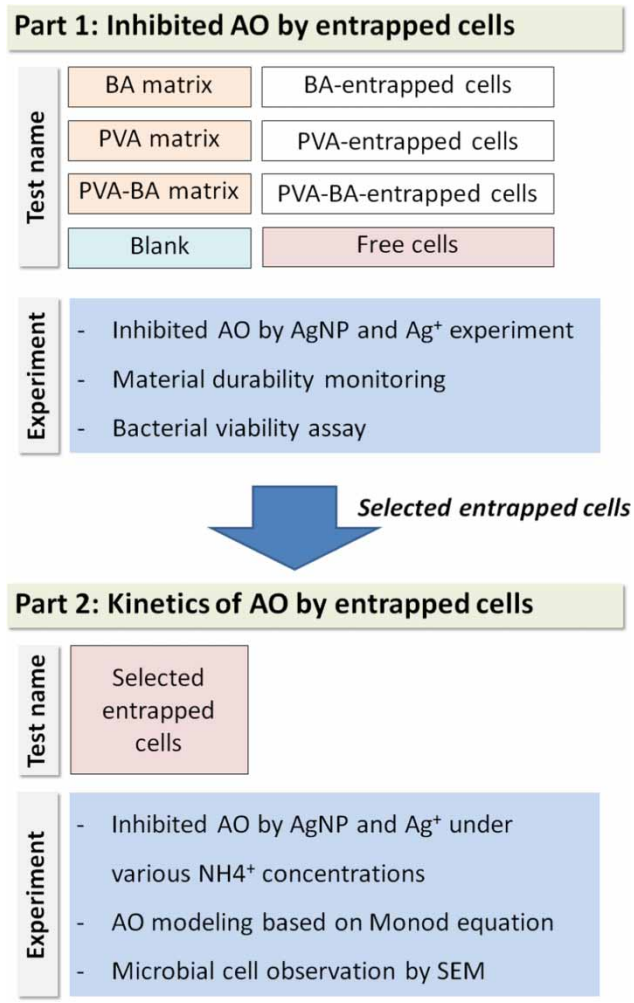

Figure 1 | Experimental procedure for AO by entrapped and free cells under presence of silver.

$NH4^+$-N concentration was selected following the concentrations reported in municipal wastewater (Bai *et al.* 2012). The Ag^+ and AgNP concentrations were chosen based on the inhibition information reported previously (Giao *et al.* 2017). In the previous work, AO with AgNP concentrations of 0, 1, 10, and 100 mg/L was tested. The tests with AgNPs of 10 and 100 mg/L gave similar inhibition (63 and 76% compared to the test without AgNP, respectively). Therefore the AgNP concentration at 10 mg/L was chosen for this study. The selected Ag^+ concentration (0.1 mg/L) was the released concentration from 10 mg/L AgNP suspension (Giao *et al.* 2017). A nitrifying sludge of 50 mg-MLSS/L was used. The AO experiments were conducted with cells entrapped in BA, PVA, and PVA-BA. 100 mL of the reactor with different entrapped cells was aerated to obtain DO at 2 mg/L. Water samples were taken after a 60-h test. The

Downloaded from http://iwaponline.com/wst/article-pdf/79/5/1007/618293/wst079051007.pdf
by guest

selected period (60 hour) was preliminarily tested and AO had completely reached a plateau (the preliminary result shown in Figure S1 in the supplementary material, available with the online version of this paper). Inhibition percentage of AO was estimated and compared to the reactors without silver. The inhibition percentage of AO activity was calculated based on Equation (1).

$$\text{Inhibition } (\%) = \frac{AR_C - AR_i}{AR_C} \times 100 \quad (1)$$

where AR_C is the percentage of ammonia reduction in the controls (free or entrapped cell reactor with no silver) and AR_i is percentage of ammonia reduction under the presence of AgNPs or Ag^+.

Kinetics of AO by selected entrapped cells

For the kinetic experiments, the 60-h AO tests with NH_4^+-N (10 to 180 mg-N/L) and silver (AgNPs of 10 mg/L, Ag^+ of 0.1 mg/L, and no silver addition) were performed. The NH_4^+-N concentrations were selected to represent the concentrations reported in municipal and industrial wastewater, such as coking and rubber production wastewater (Limpiyakorn *et al.* 2005; Chaiprapat & Sdoodee 2007; Bai *et al.* 2012). The selected silver concentrations previously reported a similar AO inhibition percentage from the free nitrifying sludge (Giao *et al.* 2017). 100 mL of the reactors and the selected entrapped and free cells were aerated for 60 h. The aqueous samples were collected at 0, 5, 17, 42, and 60 h to monitor AO rate. The concentration of NH_4^+-N was measured using the salicylate–hypochlorite method (Bower & Holm-Hansen 1980). The $NH4^+$-N measurement method was selected because it is more suitable when several ions, such as Ca^{2+}, Mg^{2+}, and Cl^-, are present in the sample (Le & Boyd 2012). This method is frequently used for the analysis of ammonia in seawater.

The NH_4^+-N concentration was used to calculate the AO rate and kinetics. Reduction of NH_4^+-N concentration was plotted versus time to calculate the AO rate in mg-N/L/h. The specific AO (q) was estimated as follows in Equation (2).

$$q = \frac{1}{X} \cdot \frac{dS}{dt} \quad (2)$$

where q is the specific AO rate (mg-N/g-MLSS · h), X is the initial biomass concentration applied in this study (mg-MLSS/L), S is the initial NH_4^+-N concentration (mg/L), and t is the time elapsed during the AO experiment (h).

The specific AO rate was then calculated for the kinetic parameters based on the Monod model. The traditional Monod equation depends on microbial growth. However, in this study, the microbial cells were entrapped in the matrices. Thus, the modified Monod equation based on substrate utilization was applied. Theoretically, the Monod model cannot directly be applied under inhibitory conditions. In previous work, an uncompetitive-like inhibition model was proposed (Giao *et al.* 2017). The q and the half-saturation constant (or Monod constant) for AO (K_s) were calculated based on the inhibitory constant (K_i) and the inhibitor concentration (I), as presented in Equation (3). To determine K_i, experiments under various inhibitor concentrations were required. In this study, the focus was only on the treatment by different entrapped cells. Therefore, complete uncompetitive-like kinetics of AO under the presence of silver species might be further investigated. In this study, the apparent specific AO rate (q') and half-saturation constant (K'_S) for AO were proposed (Equation (4)).

$$q = \frac{(q_{\max}/(1 + (I/K_i))) \cdot S}{K_s/(1 + (I/K_i)) + S} \quad (3)$$

$$q' = \frac{q'_{\max} S}{K'_s + S} \quad (4)$$

q' and $q'_{\max}$ are the apparent specific AO rate and the apparent maximum specific AO rate (mg-N/g-MLSS · h), respectively. K'_s is the apparent half-saturation constant (or Monod constant) for AO (mg/L). For estimation of the kinetic parameters, $q'_{\max}$ and K'_s were calculated using a linear plot that followed the Lineweaver-Burk equation (Equation (5)). Triplicate experimental data were used for kinetic parameter estimation. Experimental and model data were statistically confirmed by non-linear regression analysis using Sigma Plot software provided by Khon Kaen University, Thailand (R^2 of 0.86–0.96, $p < 0.0001$).

$$\frac{1}{q'} = \frac{K'_s}{q'_{\max}} \cdot \frac{1}{S} + \frac{1}{q'_{\max}} \quad (5)$$

Free and entrapped cell viability using live/dead assay

Free and entrapped cell viability was investigated. Ten entrapped cell beads after the experiment were collected. The bead sample was washed five times with de-ionized water and five times with a NaCl solution (0.85%). The washed beads were cut using a pair of tweezers. The tweezed beads were dipped in 10 mL of NaCl (0.85%) and

Downloaded from http://iwaponline.com/wst/article-pdf/79/5/1007/618293/wst079051007.pdf
by guest

then gently squeezed to let the cells out of the entrapment matrices. The suspended cells (free and de-entrapped cells) were centrifuged at 5,000 rpm for 5 min. The supernatant was discarded, and the pellets were collected. The pellets were re-suspended and concentrated to obtain the free and de-entrapped cell samples for the live/dead assay.

The staining procedure was performed using a staining kit (LIVE/DEAD® BacLight™ Bacterial Viability, Molecular Probes, Invitrogen). The samples were observed under CLSM (FluoView FV10i, Olympus, Japan). The following two samples were compared: (1) microbial cells directly taken from the nitrifying reactor and (2) killed cells (autoclaved at 121 °C, at 100 kPa for 15 min), stained for estimation of microbial viability. The percentage of live and dead cells was estimated based on 30 CLSM-images. The results were presented as % dead cells (±standard deviation).

Scanning electron microscopic observation

After the kinetic experiment, microbial cells and bead physiology were observed using SEM-EDX. The BA-entrapped cells (selected matrix) were prepared for SEM observations according to the procedure by Siripattanakul-Ratpukdi *et al.* (2014). Briefly, the entrapped cell beads from the experiment were collected and washed with de-ionized water. The collected gel beads were fixed using 1% osmium tetroxide for 1 h. The fixed gel beads were then rinsed three times with de-ionized water for 10 min. The beads were dehydrated with a series of ethanol that ranged from 30 to 95%. The absolute ethanol was applied as the last step of the dehydration. The dehydrated beads were dried using a critical point dryer (Balzers, CPD 020, Liechtenstein). The beads were divided into two parts using a razor blade in liquid nitrogen, attached to a stub, and coated with gold. The dried BA, PVA, and PVA-BA beads were observed using SEM with an energy-dispersive spectroscopy attachment (JEOL, JSM-5410LV, Tokyo, Japan). Elemental compositions of selected areas were analyzed using an energy dispersive X–ray (EDX, Oxford Instruments, Model X–MaxN, UK) to identify aggregates of silver.

Statistical analysis

The percentage of AO inhibition and membrane compromised cells caused by AgNPs and Ag^+ was presented as an averaged percent inhibition (%) ±standard deviation (SD), regardless of the initial NH_4^+–N concentrations. A statistical comparison was performed using IBM SPSS statistics for Windows, Version 19.0 (IBM Corp., Armonk, NY, USA). The significance of the differences ($p < 0.05$) was determined by a one-way analysis of variance (ANOVA) followed by Duncan's test (Ahrari *et al.* 2015).

RESULTS AND DISCUSSION

Inhibited AO by entrapped cells

Percentage of AO inhibition

An AO experiment under various conditions was performed. Blank AO test and AO tests by only entrapment matrices (no cells) were conducted (results presented in Figure S2 in the supplementary material, available with the online version of this paper). It was found that natural ammonia removal (based on blank experiment) and ammonia adsorption on entrapment matrices did not obviously occur. For the tests with nitrifying sludge, under the absence of silver contamination, the nitrifying sludge reduced ammonia. Percentages of AO by the free (94.5%) and entrapped (90.2–95.5%) nitrifying sludge were similar (Figure 2). The entrapped cells did not run into limited substrate diffusion problem (Siripattanakul-Ratpukdi *et al.* 2014). This showed potential of entrapped cell utilization in the future.

During the experiments with silver, AO performance was significantly reduced. Under the presence of AgNP (10 mg/L), the free and entrapped cells reduced ammonia by 31.3 and 55.0–70.2%, respectively. With regards to the influence of Ag^+ (0.1 mg/L), the free and entrapped cells oxidized ammonia by 19.4 and 54.2–75.5%, respectively. Previously, Giao *et al.* (2017) reported that the AO inhibition by silver caused by microbial cell damage. In this study, the entrapment matrix led to tortuosity of silver to reach to

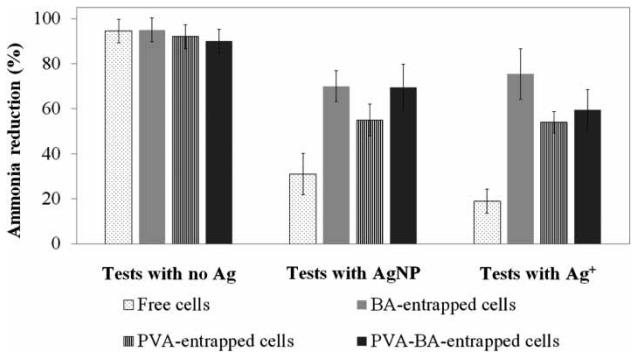

Figure 2 | Percentages of AO by the free and entrapped cells (BA, PVA, and PVA-BA) under the absence (Ag 0 mg/L) and presence of silver species (AgNPs 10 mg/L and Ag^+ 0.1 mg/L) after the 60-h experiment. The error bar indicates the standard deviation.

Downloaded from http://iwaponline.com/wst/article-pdf/79/5/1007/618293/wst079051007.pdf
by guest

Table 1 | Inhibition percentage of AO caused by AgNPs and Ag^+

Microorganism	Silver species and concentration	Inhibition percentage of AO (%)	Reference
BA-entrapped nitrifying sludge	AgNPs at 10 mg/L	20.8	This study
BA-entrapped nitrifying sludge	Ag^+ at 0.1 mg/L	15.0	This study
Free nitrifying sludge	AgNPs at 10 mg/L	63.3	Giao *et al.* (2017)
Free nitrifying sludge	Ag^+ at 0.1 mg/L	75.3	Giao *et al.* (2017)
Calcium alginate-entrapped nitrifying sludge	AgNPs at 5 mg/L	19.0–35.0	Siripattanakul-Ratpukdi *et al.* (2014)
PVA-entrapped nitrifying sludge	AgNPs at 1 mg/L	18.0–95.0	Siripattanakul-Ratpukdi *et al.* (2014)
Free nitrifying sludge	Ag^+ at 1 mg/L	13.5	Liang *et al.* (2010)
Free nitrifying sludge	AgNPs at 1 mg/L	41.4	Liang *et al.* (2010)
Free nitrifying sludge	AgNPs at 1 mg/L	100.0	Choi *et al.* (2009)

microbial cells resulting better AO by the entrapped cells. Figure 2 clearly shows that AgNPs at 10 mg/L and Ag^+ at 0.10 mg/L (represented liberated dissolved silver from AgNPs) partially inhibited AO of the BA-entrapped cells by 25.4 and 19.4%, the PVA-entrapped cells by 37.0 and 38.2%, and the PVA-BA-entrapped cells by 20.7 and 30.4%, respectively. The result revealed that the BA and PVA-BA-entrapped cells performed better than the PVA-entrapped cells. The different entrapment materials produced different gel structures resulting in altered AO inhibition. When compared to the result of free cells reported previously, inhibition percentages of AO by AgNPs at 10 mg/L and Ag^+ at 0.10 mg/L were 63.3% and 75.3%, respectively (Table 1). The results clearly showed lower AO inhibition in the entrapped cell experiment.

We preliminarily monitored NO_2^- plus NO_3^--N concentration during the experiments as shown in Table S1 (in supplementary material, available online). The result stated that the entrapment material (BA) did not show the ammonia removal and nitrite plus nitrate production. Nitrite plus nitrate accumulated in all tests with microbial cells under the presence or the absence of silver. However, it was obvious that silver influenced AO and nitrite plus nitrate production. At AgNPs 10 mg/L and Ag+ 0.10 mg/L, inhibition of nitrite plus nitrate production was 41% and 56%, respectively.

Durability of entrapped cells

In this sub-section, the stability of the entrapped cell beads was the focus. Only the durability of the entrapped beads after 30 days of exposure to AgNPs and Ag^+ was observed. Figure 3 preliminarily indicates the durability of the gel beads. During the experiment, damaged beads were quantified based on bead swelling and abrasion compared to beads at the beginning. After 30 days, no damaged BA beads (0%) were observed while the PVA (56%) and PVA-BA (10%) beads were obviously swollen and damaged. This phenomenon was also reported in a previous study (Bach & Dinh 2014). The PVA beads deformed because of the hydrophilic nature. The cross-linking of PVA and boric acid could be reversed, resulting in bead swelling. The results revealed that the addition of

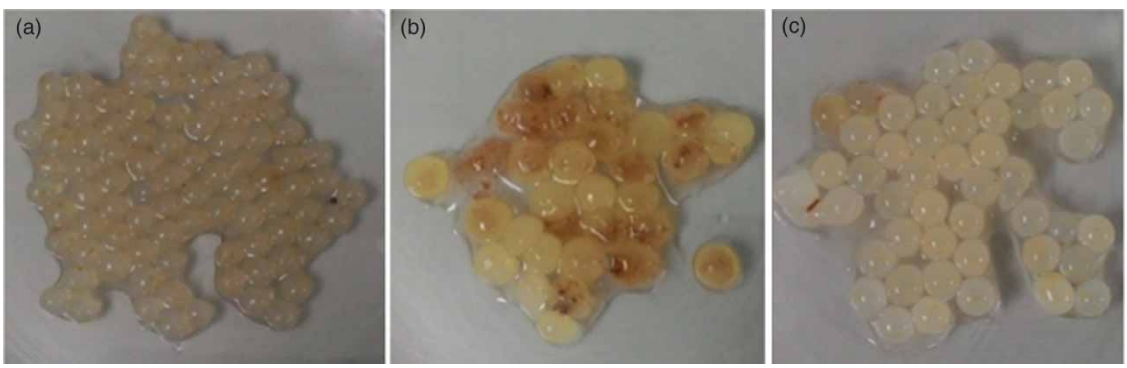

Figure 3 | Sludge entrapped in (a) BA, (b) PVA, and (c) PVA-BA after shaking for 30 days at 200 rpm with AgNPs at 10 mg/L.

Downloaded from http://iwaponline.com/wst/article-pdf/79/5/1007/618293/wst079051007.pdf
by guest

BA into the PVA gel could improve stability in SWW. This result was in line with other studies that showed that a combination of PVA and BA led to higher stability and storage longevity of the produced gel beads (Paul & Vignais 1980; Liu *et al.* 2012). Among the cell entrapment techniques, the BA-entrapped cells were the most stable beads. Similarly, a previous study reported that BA had high gel strength and flexibility (Taweetanawanit *et al.* 2017). The BA-entrapped cells were stable during long-term operation and supported the growth of the entrapped microbes (Siripattanakul-Ratpukdi & Tongkliang 2012).

The cell viability assay (after the 60-h experiment), based on bacterial cell membrane damage is shown in Figure 4. The proportions of dead cells between the free cells (collected directly from the enriching reactor) and the controlled BA- and PVA-entrapped cells (entrapped cells without AgNPs or Ag^+ exposure) were insignificantly different ($p > 0.05$). The result revealed that BA and PVA were not toxic to bacterial cells. Prior studies reported that BA and PVA were not harmful to microbes (Siripattanakul & Khan 2010; Wadhawan *et al.* 2011; Vecchiatini *et al.* 2015).

Conversely, the percentage of dead cells from the PVA-BA-entrapped cell test (no silver) was significantly higher than free cells ($p < 0.05$). As discussed earlier, BA and PVA are non-toxic to microbial cells, and likewise the mixture of PVA-BA should not cause toxicity to the entrapped cells. The damaged cells in the PVA-BA test might be due to the viscosity of the material (PVA-BA) resulting in less diffusion of oxygen and ammonia (substrate) into the beads. Among the entrapped cells, BA was the most promising entrapment material for mitigation of the toxicity of AgNPs and Ag^+. The BA matrix promoted high treatment performance (low inhibition) and cell viability.

Kinetics of AO by BA-entrapped cells

The kinetics of AO from the BA-entrapped cells are demonstrated in Figure 5. Table 2 is a summary of the AO kinetic parameters. Figure 5 shows that the experimental results well fitted Monod model. Under absence of silver, self-substrate inhibition did not occur, resulting in the steady specific AO rates for the tests with NH_4^+ higher than 100 mg/L. Based on free ammonia calculation, only 0.56 mg/L free ammonia may form (Anthonisen *et al.* 1976). Free ammonia of 10–150 mg/L could inhibit AO. At the concentration related to this study, no inhibition by free ammonia would take place. The result from this study revealed that the tested NH_4^+ concentrations (0–180 mg-N/L) did not show adverse effect from nitrogenous species.

Results from the tests with no silver indicated that the entrapped cell system encountered the substrate diffusion problem resulting in much lower q_{max} values compared to that of the free cells. Under the presence of silver, both K'_S and q'_{max} values of the free cell systems were much lower than those without silver. This result implied that inhibitors (AgNPs or Ag+) obviously influenced AO in the free cell system. The entrapped cell tests with silver (both species) had similar kinetic parameter values (Table 2). This highlights the success of the cell entrapment application for reducing AgNPs and liberated Ag^+ toxicity. Table 1 confirms that the entrapped cells reduced the influence of AgNPs and Ag^+ by three and five times, respectively, as compared to those from the suspended cells at the same conditions.

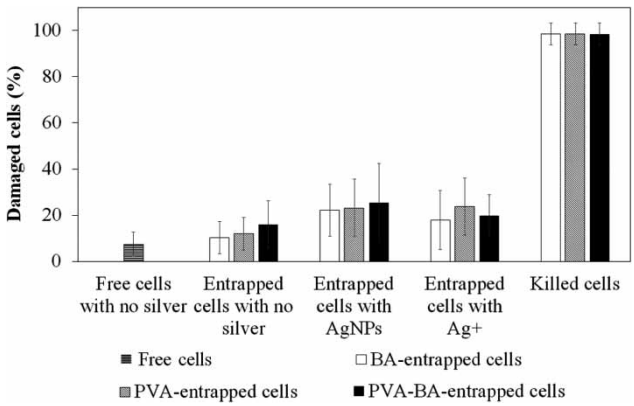

Figure 4 | Percentage of damaged cells from the tests with non-inhibited free cells (free cells with no Ag), non-inhibited entrapped cells (entrapped cells with no Ag), inhibited entrapped cells by 10 mg/L of AgNPs (entrapped cells with AgNPs) and 0.1 mg/L of Ag^+ (entrapped cells with Ag^+). Error bars indicate the standard deviation.

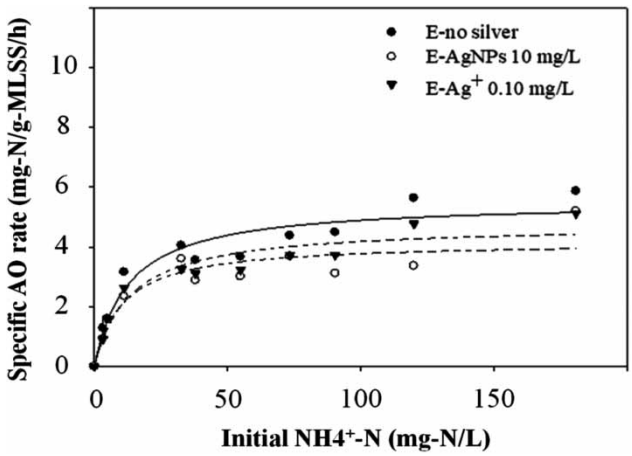

Figure 5 | Kinetics of AO by the nitrifying sludge entrapped in BA with no silver (•), AgNPs at 10 mg/L (○), and Ag^+ at 0.1 mg/L (▾).

Downloaded from http://iwaponline.com/wst/article-pdf/79/5/1007/618293/wst079051007.pdf
by guest

Table 2 | AO kinetic parameters under the absence and presence of silver

Cell mode	Silver species and concentration	Kinetic parameters	
Test with no silver		K_s (mg/L)	q_{max} (mg-N/g-MLSS · h)
Free cells	No silver	17.8[a]	12.8[a]
BA-entrapped cells	No silver	12.9	5.6
Test with silver		K'_s (mg/L)	q'_{max} (mg-N/g-MLSS · h)
Free cells	AgNPs at 10 mg/L	3.3[a]	3.3[a]
	Ag^+ at 0.1 mg/L	3.7[a]	1.3[a]
BA-entrapped cells	AgNPs at 10 mg/L	10.5	4.2
	Ag^+ at 0.1 mg/L	13.4	4.8

[a]Results from Giao *et al.* (2017).

Microscopic observation of BA-entrapped cells

Figure 6 presents SEM images of the BA-entrapped cells. As shown in Figure 5(a) and 5(b), several micro-colonies laid on the BA-matrices. A previous study indicated that cross-linking between barium and alginate created a dense network with an abundance of fine pores (Siripattanakul-Ratpukdi & Tongkliang 2012). This study also found numerous small pores (Figure 6(c)). The pore sizes ranged from 0.1 to 0.3 μm, which were much smaller than the single cells (1–2 μm), resulting in no micro-colonies in the pores. The small porous structure was related to the low maximum

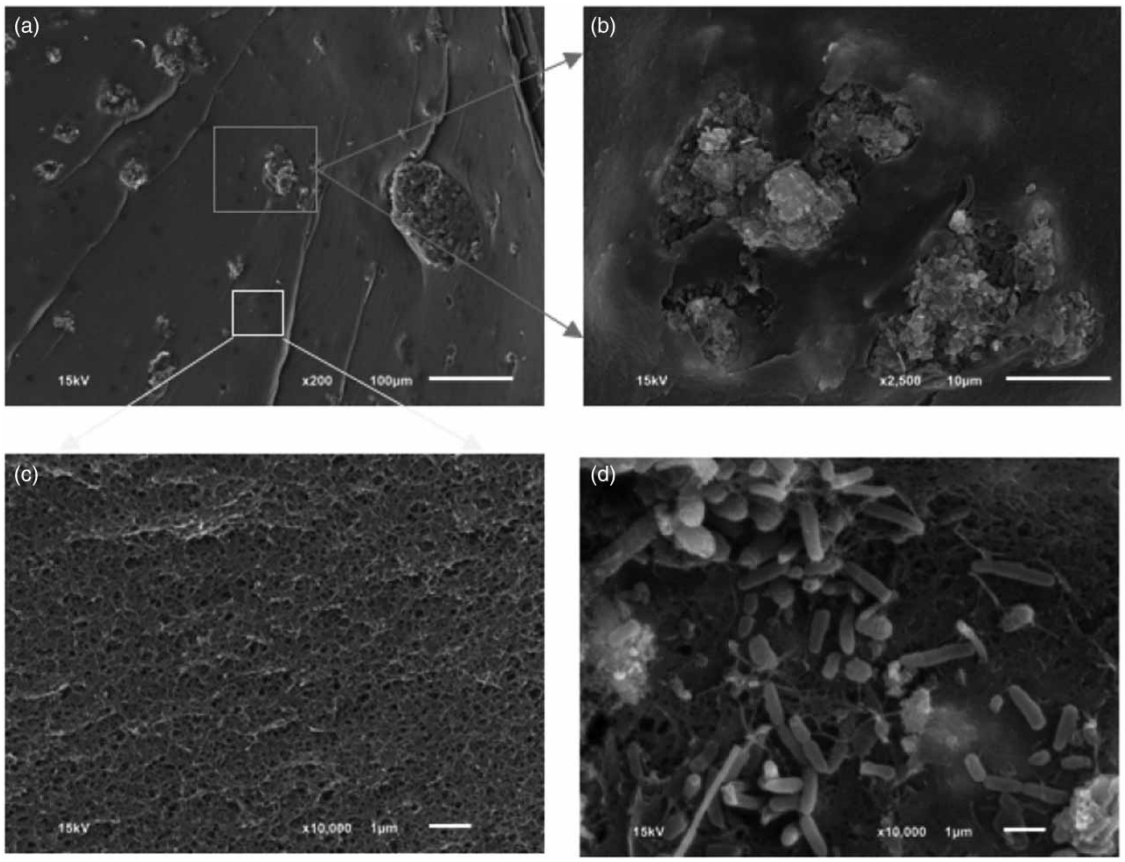

Figure 6 | SEM micrographs for observation of BA-entrapped cells after 60 h of exposure to AgNPs at 10 mg/L. (a) Cross-section of the BA-entrapped beads with several colonies of cells found in the BA matrices, observed at 200×. (b) Microbial cells were surrounded by BA-matrices, observed at 2,500×. (c) The microporous structures formed by ionic-cross linking between alginate and barium ions. The sizes of the pores were estimated as 0.1–0.3 μm, observed at 10,000×. (d) A cluster of cells with long- (majority) and short-rod (minority) shapes, observed at 10,000×.

Downloaded from http://iwaponline.com/wst/article-pdf/79/5/1007/618293/wst079051007.pdf
by guest

AO rates found in the kinetic experiment of the entrapped cells. This structure was torturous for the substrate to reach the microbial cells inside the BA beads. The dense structure protected the cells from silver species, leading to similar AO rates in the experiments by the entrapped cells under absence and presence of silver species.

It was noted by Giao *et al.* (2017) that the microbial cells changed from long rod-shaped to shorter rod-shaped in the presence of AgNPs. In this study, most of the cells remained long rod-shaped (Figure 6(d)). This could primarily indicate that the microbial cells were not stressed from the toxic substance; therefore, cell morphological adaptation was not observed. During SEM observation, element (silver) analysis using an EDX technique was also performed. In the entrapped cell experiment, silver clusters were not detected inside the beads. This confirmed that the entrapment matrices reduced AgNPs and liberated Ag^+ transporting into the beads.

CONCLUSION

The entrapment materials, including BA, PVA, and PVA-BA, were non-toxic to microbial cells. In the short-term AO test, BA was the most promising entrapment material for reduction of AgNPs and Ag^+ toxicity. The inhibitory kinetics results showed that the cells entrapped in BA maintained high microbial cell viability (approximately 20% dead cells) and AO up to 90% in the presence of AgNPs or Ag^+. The kinetic parameters confirmed low influence of AgNPs and Ag^+ on AO by the entrapped cells. Microscopic observation of the entrapped cells suggested that the porous structure of matrices limited penetration of silver, resulting in lower cell damage and AO inhibition. Future study on the long-term impact of AgNPs and Ag^+ on AO activity and microbial community change in entrapped cells should be investigated.

ACKNOWLEDGEMENTS

The authors acknowledge financial and equipment support from the Research Center for Environmental and Hazardous Substance Management (Khon Kaen University) and Research Career Development Grant RSA6080054 (Thailand Research Fund (TRF) and Khon Kaen University). This work was supported by the National Nanotechnology Center (NANOTEC), NSTDA, Ministry of Science and Technology, Thailand, through its program of Research Network NANOTEC (RNN). Any opinions, findings, and conclusions or recommendations expressed in this material are those of the authors and do not necessarily reflect the views of the grant agencies.

REFERENCES

Ahrari, F., Eslami, N., Rajabi, O., Ghazvini, K. & Barati, S. 2015 The antimicrobial sensitivity of *Streptococcus mutans* and *Streptococcus sangius* to colloidal solutions of different nanoparticles applied as mouthwashes. *Dental Research Journal* **12** (1), 44–49.

Anthonisen, A. C., Loehr, R. C., Prakasam, T. B. S. & Srinath, E. G. 1976 Inhibition of nitrification by ammonia and nitrous acid. *Journal of the Water Pollution Control Federation* **48** (5), 835–852.

Bach, L. T. & Dinh, P. V. 2014 Immobilized bacteria by using PVA (polyvinyl alcohol) crosslinked with sodium sulfate. *International Journal of Science and Engineering (IJSE)* **7** (1), 41–47.

Bai, Y., Sun, Q., Wen, D. & Tang, X. 2012 Abundance of ammonia-oxidizing bacteria and archaea in industrial and domestic wastewater treatment systems. *FEMS Microbiology Ecology* **80** (2), 323–330.

Bower, C. E. & Holm-Hansen, T. 1980 A salicylate-hypochlorite method for determining ammonia in seawater. *Fishery and Aquaculture Science* **37**, 794–798.

Chaiprapat, S. & Sdoodee, S. 2007 Effects of wastewater recycling from natural rubber smoked sheet production on economic crops in southern Thailand. *Resources, Conservation and Recycling* **51**, 577–590.

Choi, O., Deng, K. K., Kim, N. J., Ross, J., Surampallie, R. Y. & Hua, Z. 2008 The inhibitory effects of silver nanoparticles, silver ions, and silver chloride colloids on microbial growth. *Water Research* **42**, 3066–3074.

Choi, O., Cleuenger, T., Deng, B., Surampalli, R., Ross, L. & Hu, Z. 2009 Role of sulfide and ligand strength in controlling nanosilver toxicity. *Water Research* **43**, 1879–1886.

Chopra, I. 2007 The increasing use of silver-based products as antimicrobial agents: a useful development or a cause for concern. *Journal of Antimicrobial Chemotherapy* **59**, 587–590.

Giao, N. T., Limpiyakorn, T., Kunapongkiti, P., Thuptimdang, P. & Siripattanakul-Ratpukdi, S. 2017 Influence of silver nanoparticles and liberated silver ions on nitrifying sludge: ammonia oxidation inhibitory kinetics and mechanism. *Environmental Science and Pollution Research* **24** (10), 9229–9240.

Hoque, M. E., Khosravi, K., Newman, K. & Metcalfe, C. D. 2012 Detection and characterization of silver nanoparticles in aqueous matrices using asymmetric-flow field flow fractionation with inductively coupled plasma mass spectrometry. *Journal of Chromatography A* **1233**, 109–115.

Hu, J. & Yang, Q. 2015 Microbial degradation of di-*N*-butylphthalate by *Micrococcus* sp. immobilized with polyvinyl alcohol. *Desalination and Water Treatment* **56**, 2457–2463.

Downloaded from http://iwaponline.com/wst/article-pdf/79/5/1007/618293/wst079051007.pdf
by guest

Jeong, E., Chae, S. R., Kang, S. T. & Shin, H. S. 2012 Effects of silver nanoparticles on biological nitrogen removal processes. *Water Science and Technology* **65** (7), 1298–1303.

Le, P. T. T. & Boyd, C. E. 2012 Comparison of phenate and salicylate methods for determination of total ammonia nitrogen in freshwater and saline water. *Journal of the World Aquaculture Society* **43** (6), 885–889.

Li, L., Hartmann, G., Döblinger, M. & Schuster, M. 2013 Quantification of nanoscale silver particles removal and release from municipal wastewater treatment plants in Germany. *Environmental Science and Technology* **47**, 7317–7323.

Liang, Z., Das, A. & Hu, Z. 2010 Bacterial response to a shock load of nanosilver in an activated sludge treatment system. *Water Research* **44**, 5432–5438.

Limpiyakorn, T., Shinohara, Y., Kurisu, F. & Yagi, O. 2005 Communities of ammonia-oxidizing bacteria in activated sludge of various sewage treatment plants in Tokyo. *FEMS Microbiology Ecology* **54** (2), 205–217.

Liu, Z.-Q., Zhou, M., Zhang, X.-H., Xu, J.-M., Xue, Y.-P. & Zheng, Y.-G. 2012 Biosynthesis of iminodiacetic acid from iminodiacetonitrile by immobilized recombinant *Escherichia coli* harboring nitrilase. *Journal of Molecular Microbiology and Biotechnology* **22**, 35–47.

Lucchesi, G. I., Bergero, M. F., Boeris, P. S., López, G. A., Heredia, R. M. & Liffourrena, A. S. 2015 Immobilization of *P. putida* a (ATCC 12633) cells using Ca-alginate: environmental applications for the removal of cationic surfactants pollutants in industrial wastewater. *Alginic Acid: Chemical Structure, Uses and Health Benefits* **2015**, 105–118.

Mitrano, D. M., Lesher, E. K., Bednar, A., Monserud, J., Higgins, C. P. & Ranville, J. F. 2011 Detecting nanoparticulate silver using single-particle inductively coupled plasma-mass spectrometry. *Environmental Toxicology and Chemistry* **31**, 115–121.

Pantic, I. 2014 Application of silver nanoparticles in experimental physiology and clinical medicine: current status and future prospects. *Reviews on Advanced Materials Science* **2014** (37), 15–19.

Paul, F. & Vignais, P. M. 1980 Photophosphorylation in bacterial chromatophores entrapped in alginate gel: improvement of the physical and biochemical properties of gel beads with barium as gel-inducing agent. *Enzyme and Microbial Technology* **2** (4), 281–287.

Saez, J. M., Benimeli, C. S. & Amoroso, M. J. 2012 Lindane removal by pure and mixed cultures of immobilized actinobacteria. *Chemosphere* **89**, 982–987.

Siripattanakul, S. & Khan, E. 2010 Fundamentals and applications of entrapped cell bioaugmentation for contaminant removal. *Emerging Environmental Technologies* **2**, 147–170.

Siripattanakul-Ratpukdi, S. 2012 Entrapped cell system for decentralized hospital wastewater treatment: inhibitory effect of disinfectants. *Environmental Technology* **33** (20), 2319–2328.

Siripattanakul-Ratpukdi, S. & Tongkliang, T. 2012 Municipal wastewater treatment using barium alginate entrapped activated sludge: adjustment of utilization conditions. *International Journal of Chemical Engineering and Applications* **3** (5), 328–332.

Siripattanakul-Ratpukdi, S., Ploychankul, C., Limpiyakorn, T., Vangnai, A. S., Rongsayamanont, C. & Khan, E. 2014 Mitigation of nitrification inhibition by silver nanoparticles using cell entrapment technique. *Journal of Nanoparticle Research* **16**, 2218.

Taweetanawanit, P., Radpukdee, T., Giao, N. T. & Siripattanakul-Ratpukdi, S. 2017 Mechanical and chemical stabilities of barium alginate gel: influence of chemical concentrations. *Key Engineering Materials* **718**, 62–66.

Vecchiatini, R., Penolazzi, L., Lambertini, E., Angelozzi, M., Morganti, C., Mazzitelli, S., Trombelli, L., Nastruzzi, C. & Piva, R. 2015 Effect of dynamic three-dimensional culture on osteogenic potential of human periodontal ligament-derived mesenchymal stem cells entrapped in alginate microbeads. *Journal of Periodontal Research* **50** (4), 544–553.

Wadhawan, T., Maruska, Z. B., Siripattanakul, S., Hill, C. B., Gupta, A., Prüb, B. M., McEvoy, J. M. & Khan, E. 2011 A new method to determine initial viability of entrapped cells using fluorescent nucleic acid staining. *Bioresource Technology* **102**, 1622–1627.

Wu, K.-Y. A. & Wisecarver, K. D. 1992 Cell immobilization using PVA crosslinked with boric acid. *Biotechnology and Bioengineering* **39**, 447–449.

First received 27 July 2018; accepted in revised form 10 February 2019. Available online 21 February 2019

Downloaded from http://iwaponline.com/wst/article-pdf/79/5/1007/618293/wst079051007.pdf
by guest